UCRL-11438

University of California

Ernest O. Lawrence Radiation Laboratory

A POLARIZED PROTON TARGET

Berkeley, California

Dubna Conf. Aug. 5-15, 1964

UCRL-11438

UNIVERSITY OF CALIFORNIA

Lawrence Radiation Laboratory
Berkeley, California

AEC Contract No. W-7405-eng-48

A POLARIZED PROTON TARGET

Owen Chamberlain, Claude Schultz, and Gilbert Shapiro

July 3, 1964

UCRL-11438

A POLARIZED PROTON TARGET*

Owen Chamberlain, Claude Schultz, and Gilbert Shapiro

Lawrence Radiation Laboratory
University of California
Berkeley, California

(to be presented by Herbert Steiner)

July 3, 1964

We have successfully conducted a series of experiments involving scattering of high energy pions and protons from a target containing polarized protons. Results of some of these experiments were reported at this conference, and in the literature.[1] Proton polarizations as high as 65% have been measured; the average polarization during sustained data-taking has been typically 45%.

Figure 1 shows the target material used during some of these experiments. These are crystals of lanthanum magnesium double nitrate -- $La_2Mg_3(NO_3)_{12} \cdot 24H_2O$. Protons in the water of crystallization, comprising 3% of the crystal mass, constitute the polarized sample. When the four single crystals are stacked together, they occupy roughly a 1-inch cube and weigh 26 g. Larger targets are possible, being limited at present only by the extent of the magnetic-field homogeneity. Certain experimental demands may also restrict the size of the crystal to be used.

The method used to obtain polarization of these target protons is known as "dynamic nuclear orientation", or "l'effet solide". It has been reviewed by Jeffries,[2] and by Abragam and Borghini,[3] all of whom played major roles in the development of this technique. One of us has also written a review on the subject of polarized targets.[4]

One begins by immersing the crystals in a liquid He^4 bath at a vapor pressure of less than 1 mm of mercury, yielding temperatures of 1.2°K. The apparatus is located between the pole faces of an electromagnet which provides

*Work done under the auspices of the U. S. Atomic Energy Commission.

a highly uniform field of 18.7 kOe (see Fig. 2). Under these conditions the spins of the protons, following the Boltzmann statistical distribution with respect to their magnetic energy levels, exhibit a thermal equilibrium polarization of 1/6%. Under the same conditions, entities with magnetic moments comparable to that of a free electron (660 times that of a proton) are almost completely polarized. The choice of a rare-earth crystal was made partly because the unpaired inner-shell electrons of even-atomic-number rare-earth ions can have configurations that, at these temperatures, behave as localized spin $-\frac{1}{2}$ centers having magnetic moments in excess of one Bohr magneton. For this purpose 1% of the lanthanum (which has an empty 4f-shell) is replaced by even isotopes of neodymium (with three f-electrons). This is sufficient concentration for proton polarization to take place efficiently, yet low enough that the neodymium ions constitute a dilute paramagnetic system. Other reasons for the choice of this particular target material include high hydrogen content, ease of crystal growing, and favorable ratio of relaxation rates important for the dynamical polarization process.

The crystals are located in a microwave cavity inside the helium bath, so that high-frequency radiation of the proper energy to induce "forbidden" transitions can be applied to them. In these transitions, the paramagnetic neodymium ions (hereafter called "electrons" for short) and neighboring hydrogen nuclei undergo simultaneous reversal of spin direction. The forbidden transition is made possible by weak magnetic dipolar coupling between electrons and protons, which induces mixing among the various pure Zeeman states of the electron-proton system. These levels are shown in Fig. 3.

The "allowed" transitions, in which the electron spin flips without affecting the protons, are closely coupled to the lattice vibrations. Transitions between levels connected by an allowed transition proceed very rapidly, so that the relative population of the two levels is still given essentially by the Boltzmann factor,

This means that (1) one electron is available to polarize many protons, and (2) the polarization of the electrons remains high throughout the process.

In Fig. 3 there is a calculation of the theoretically attainable proton polarizations when either of the two forbidden transitions is saturated with microwave power. Notice that (1) the amount of proton polarization theoretically attainable is characterized by capital Δ, i.e., is equal to the thermal equilibrium electron polarization, and (2) either direction of proton polarization -- parallel or anti-parallel to $\vec{H}$ -- can be obtained by means of a 0.2% change in microwave frequency, without any change in the experimental geometry.

A typical experimental geometry is shown in Fig. 4. Ten counters, labelled "alpha", are set to detect the forward-scattered particle, in coincidence with one of the ten "beta" counters, set to detect the recoil proton. In a two-body elastic scattering by a hydrogen nucleus, kinematics requires (within experimental resolution) that (1) the incident beam direction and the trajectories of the two final particles are coplanar, and (2) there is a unique correlation between the counter in which the scattered particle is detected and the counter for the corresponding recoil. Inelastic scattering and scattering from the heavy nuclei of the target material do not in general satisfy these criteria. Figure 5 shows a representation of the counting rates for each of the possible coincidences between a single alpha counter and the beta array, in one experiment. Strong peaks appear in the channel corresponding to events that satisfy the kinematic criteria. The two upper sets of data correspond to the counting rates with the two directions of target polarization, respectively. The background may be estimated either from the coincidence rate in the nonkinematic channels, or by auxiliary data taken with a dummy target containing material similar to all the elements of the polarized target except hydrogen. This auxiliary data is represented by the lowest set of data.

It is quite clear that, when we are able to detect such coincidences, the free-hydrogen elastic scatters stand out well above the background, even though hydrogen constitutes only 3% of the material in the target.

When we are unable to detect both final particles, as when one of them is unstable or has very little range, we may still try to resolve the elastic hydrogen events by using the kinematic correlation between the energy and direction of one of the final particles. Figure 6 shows that this is still possible, though not as satisfactory as in the previous case. A differential range criterion was applied to pions emerging at 90 deg in the laboratory, in a π^+-p scattering experiment at 246 MeV. The open circles and dotted curve represent data taken with a dummy target. The bump at 60 g/cm^2 corresponds to the energy of pions elastically scattered from hydrogen. A shallow bump at 90 g/cm^2 occurs at the range of the incident beam, corresponding to pions elastically scattered by heavy nuclei.

The most serious problem we have faced in the analysis of these experiments has been the accurate measurement of the amount of proton polarization in the target. We use a nuclear-magnetic-resonance (NMR) detection system, shown in Fig. 7. This system is distinguished only by its crudity. In such a large sample the NMR signal is strong, and no special sophistication is necessary to detect it. For noise suppression, we modulate the magnetic field at 400 cps by a small fraction of a line width and use this field modulation as the reference signal for a phase-sensitive detector. The signal thus detected is proportional to the derivative of the absorption (or stimulated emission) curve. Other things being equal, the size of this signal is proportional to the amount of polarization. Target polarization is defined as

$$P_T = \frac{\text{No. protons, spin up} - \text{No. protons, spin down}}{\text{No. protons, spin up} + \text{No. protons, spin down}} .$$

As a calibration point for the NMR measurement, one allows the system to come to thermal equilibrium, without microwaves, and detects a signal such as that shown in Fig. 8. The polarization corresponding to this size signal can be calculated from the known field and temperature by using the Boltzmann distribution. Figure 9 shows a similar signal, attenuated by a factor of 333, when the polarization is near 60%. One notes that there is considerable structure in these lines, and that the shape changes in going from thermal equilibrium to high polarizations. In Fig. 10, the shapes of the NMR lines have been reconstructed by integrating the previous signals numerically for (a) thermal equilibrium, (b) high positive polarization, and (c) high negative polarization. All are normalized to the same area. The shape changes because, in this highly anisotropic crystal, there are many inequivalent hydrogen sites, with different local fields. The NMR line is really a superposition of many incompletely resolved local lines. The relative spacing of these local lines is affected by the spins of the neighboring atoms, which are randomly oriented at low polarizations, but systematically aligned when the polarization is high. This alignment leads to a bunching of the local lines, leading to the asymmetric overall NMR line shown in the figures.

For a quantitative determination of the amount of polarization, a second numerical integration is performed on the reconstructed NMR line. We have built a digitizing apparatus that records the output-signal size on punched paper tape at 2-sec intervals, while the NMR frequency is swept slowly through the resonance. The double integration is performed numerically by a computer.

The location of the NMR pickup coils in the microwave cavity is shown in Fig. 11. The coils are wound in figure 8's above and below the crystals, which are not shown. The copper septum constrains the flux lines of the

oscillating field to circle it, thus providing them with a return path, and hopefully sampling the entire crystal uniformly. With such a large sample, there is likely to be a very high filling factor, so large that the level of the NMR detecting signal changes appreciably during the passage through resonance (as much as 20%). This violates the "other things being equal" qualification made earlier as to polarization measurement. One can monitor the rf level separately while sweeping through resonance, and appropriately correct the recorded signal. A more certain procedure, however, is simply to reduce the filling factor by placing the pickup leads far from the crystals, thus decreasing the rf level change due to the resonance. This leads to a poorer signal-to-noise ratio for the thermal-equilibrium signal, but an acceptable compromise has been reached.

Placing the NMR leads far from the crystals has the additional advantage that the polarizations at different points within the sample is detected with uniform sensitivity. Because of thermal gradients within the crystal, radiation damage by the beam, and surface absorption of microwaves, polarization is higher near the surface than in the interior. This effect can be determined by focusing a small beam spot on various sections of the target and observing the polarization effect in a nuclear-scattering experiment, for a given measured overall target polarization. To assure that the beam is uniformly distributed over the target in the final experiment, it is sometimes useful to defocus the beam so that a considerable fraction actually misses the target. It can be shown that if any two of the effects (beam distribution, NMR sensitivity, target polarization) is uniform throughout the sample, the measurement of the effective average target polarization will be correct.

As a further check on the calibration of the target-polarization measurement, the results of an experiment on proton-proton scattering at 315 MeV with the polarized target were compared with earlier measurements using conventional

double-scattering to determine the same parameter.[5] Agreement is good, giving us confidence in these measurements.

The polarization process requires a microwave power input of about 1W at 71 GHz. The cavity containing the crystals is not tuned, being large enough to accommodate many modes at the 4-mm wavelength used. Liquid-helium consumption is about 75 liters (at 4.2°K) per 24 hours of continuous operation. About half of this liquid helium is consumed in cooling down from 4.2°K. Transfer losses and initial cooldown of the reservoir walls account for one-third of the rest.

The direction of proton polarization can be fully reversed in about 10 min. This is done frequently as a systematic control during data-taking. Helium must be supplied about every 5 hours. About 1/2 hour is required to refill and restore full polarization. To optimize use of accelerator time, data-taking often is started before full polarization is attained, so the average polarization during such data-taking is only about 45%. As the helium level drops, heat losses decrease; so the temperature gets lower and higher polarization occurs. Under optimum conditions, after several hours of continuous polarizing, we have measured polarizations of 65%.

REFERENCES

1. O. Chamberlain, C. D. Jeffries, C. H. Schultz, G. Shapiro, and L. Van Rossum, Phys. Letters 7, 293 (1963).

2. C. D. Jeffries, Dynamic Nuclear Orientation (J. Wiley and Sons, N. Y., 1963).

3. A. Abragam and M. Borghini, in Progress in Low Temperature Physics, Vol. IV (North-Holland Press, Amsterdam, 1964).

4. G. Shapiro, in Nuclear Techniques and Instrumentation, Vol. I (North-Holland Press, Amsterdam, 1964).

5. O. Chamberlain, E. Segrè, R. Tripp, C. Wiegand and T. Ypsilantis, Phys. Rev. 105, 288 (1956).

FIGURE CAPTIONS

Fig. 1. Crystals of lanthanum magnesium double nitrate used as polarized target. The scale is in inches.

Fig. 2. Disposition of target elements between magnet pole faces.

Fig. 3. Energy-level diagram for dynamic nuclear orientation.

Fig. 4. Typical experimental geometry.

Fig. 5. Coincidence counting rate between pairs of counters, one from each array. Sharp peaks are elastic scattering from hydrogen.

Fig. 6. Scattered-pion differential-range-telescope counting rate vs amount of copper moderator, in $\pi^+ p$ elastic scattering at 246 MeV. Solid points were taken with the crystal target; open points with a dummy target.

Fig. 7. Schematic diagram of NMR system to measure polarization.

Fig. 8. Differential signal at thermal-equilibrium polarization.

Fig. 9. Differential signal at about 60% polarization.

Fig. 10. NMR line shapes, obtained by numerical integration of differential signals: (a) thermal equilibrium; (b) high positive polarization; (c) high negative polarization. All three are normalized to the same area.

Fig. 11. Cutaway drawing of microwave cavity and NMR pickup coil.

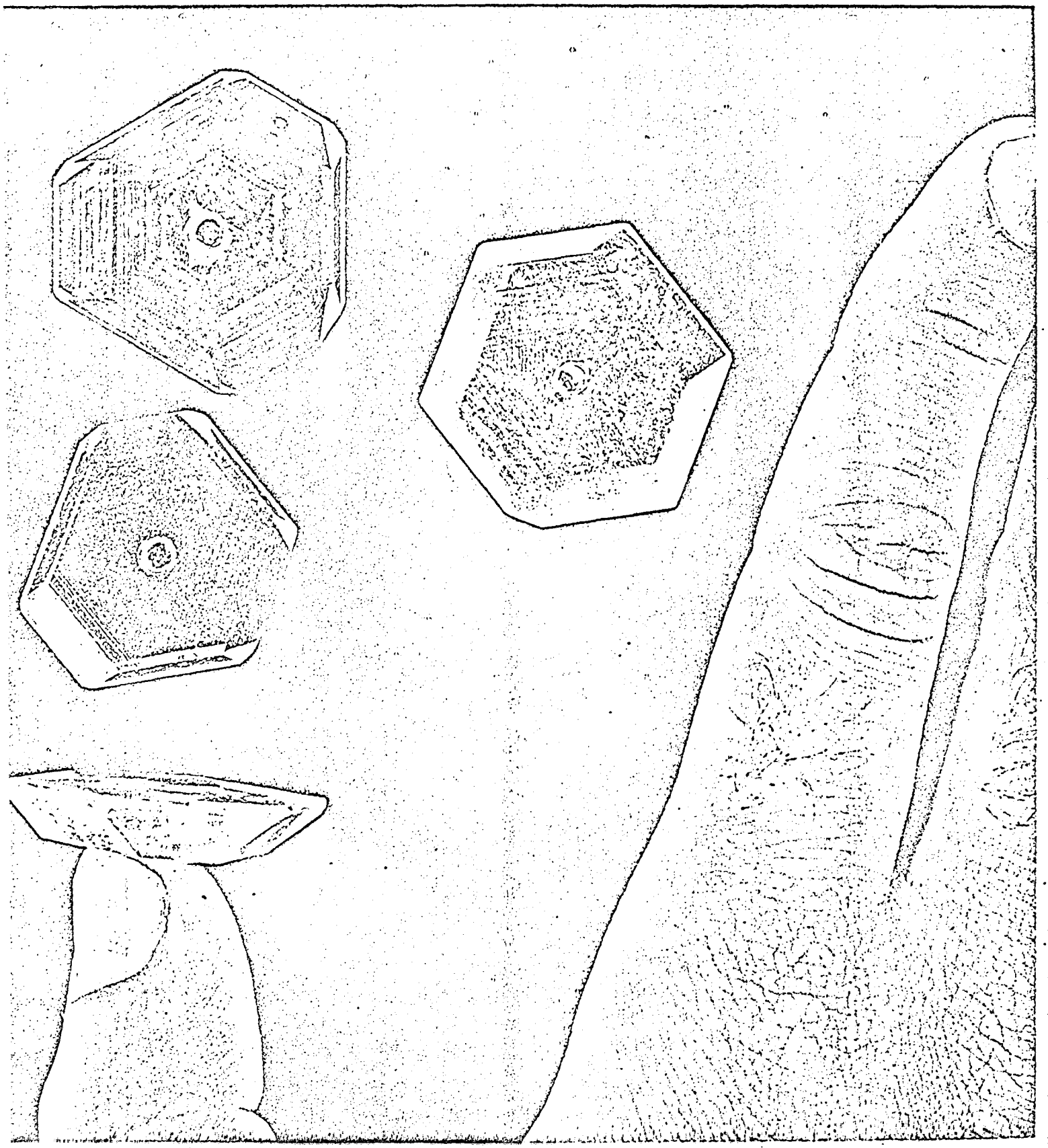

Fig. 1

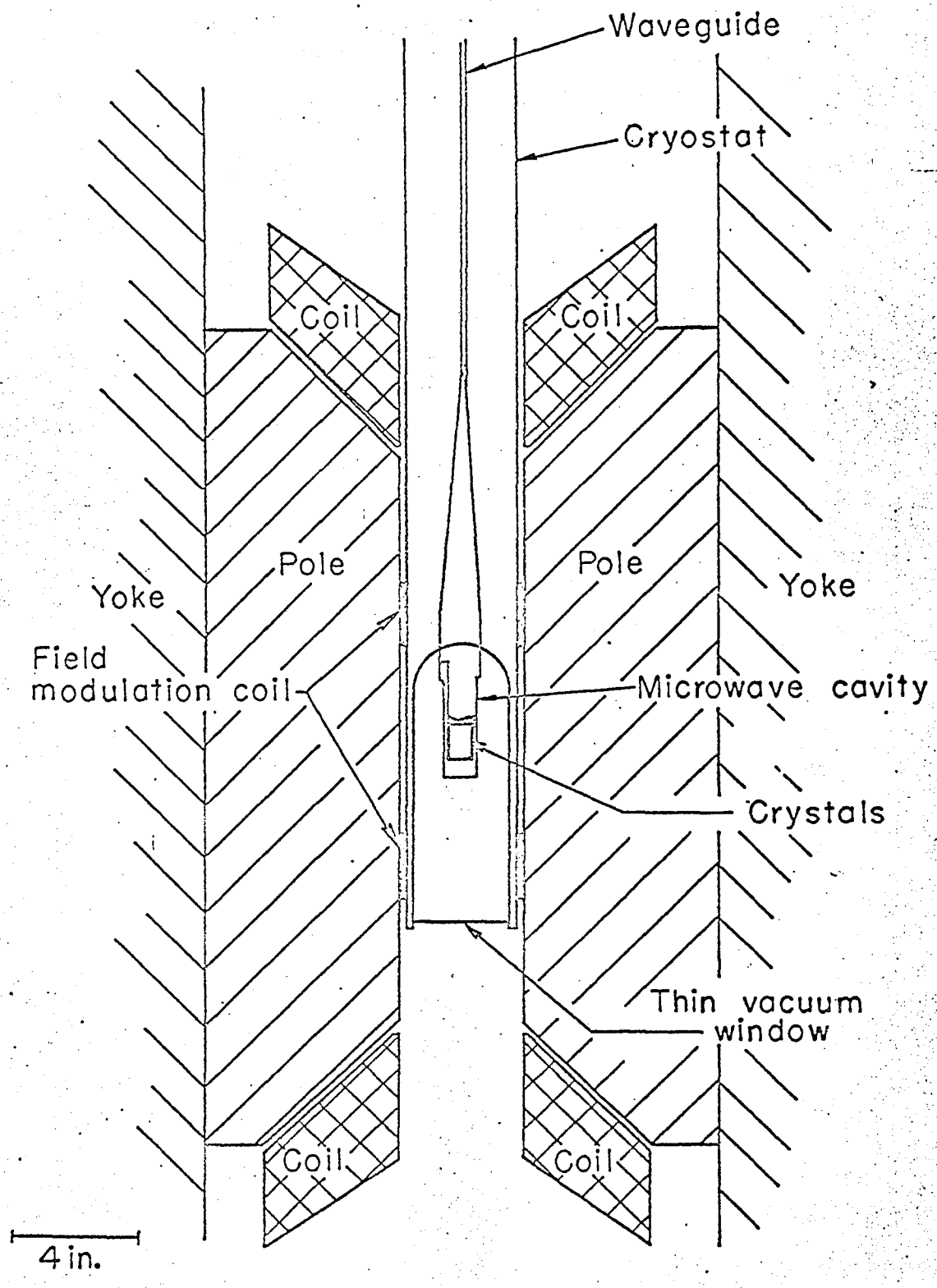

Fig. 2

MU-28649A

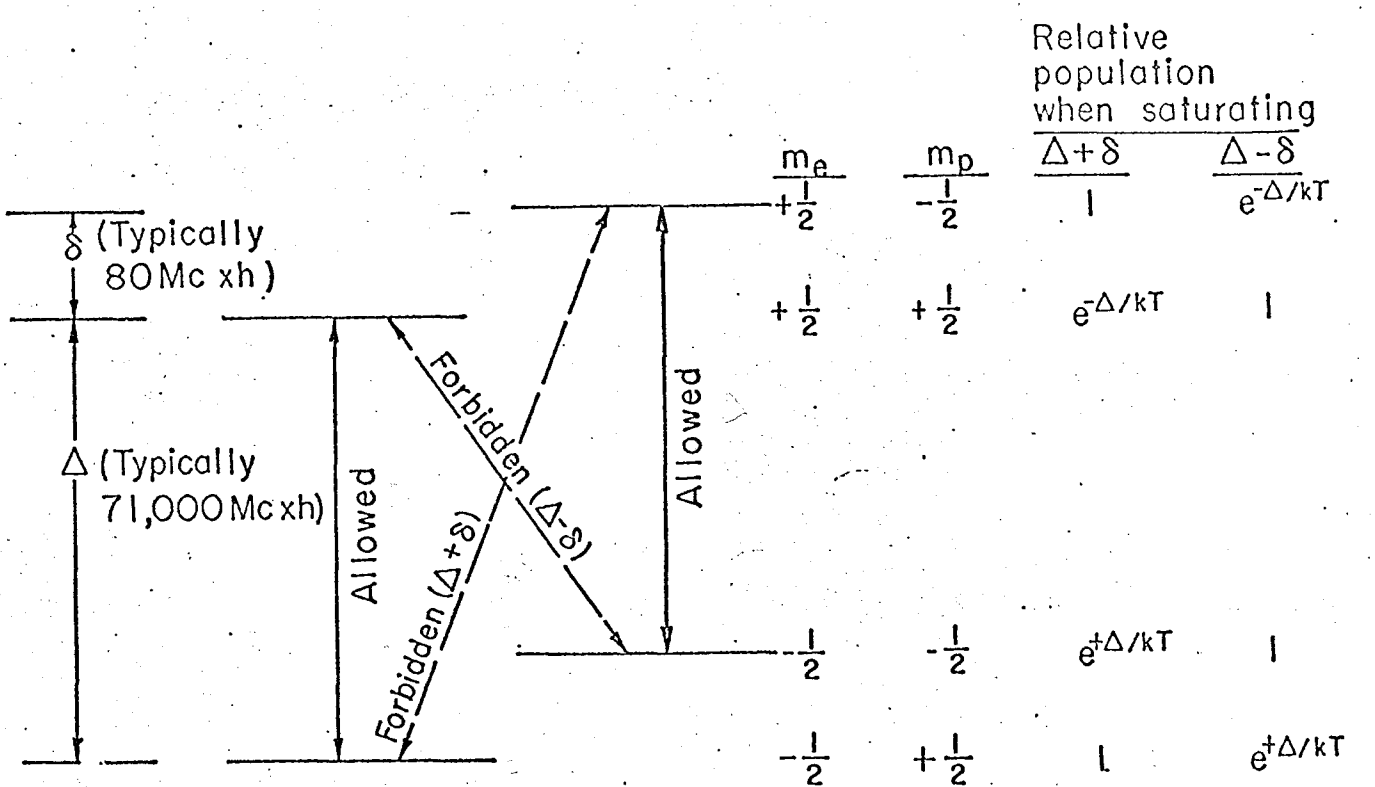

Proton polarization (saturating $\Delta+\delta$) $\longrightarrow \frac{\Sigma (m_p)_i P_i}{S \Sigma P_i} = \frac{(-\frac{1}{2})(1) + (+\frac{1}{2})(e^{-\Delta/kT}) + (-\frac{1}{2})(e^{+\Delta/kT}) + (+\frac{1}{2})(1)}{\frac{1}{2}(1 + e^{-\Delta/kT} + e^{+\Delta/kT} + 1)}$

$= -\tanh \frac{\Delta}{2kT}$

Proton polarization (saturating $\Delta-\delta$) $\longrightarrow + \tanh \frac{\Delta}{2kT}$

MU-28789

Fig. 3

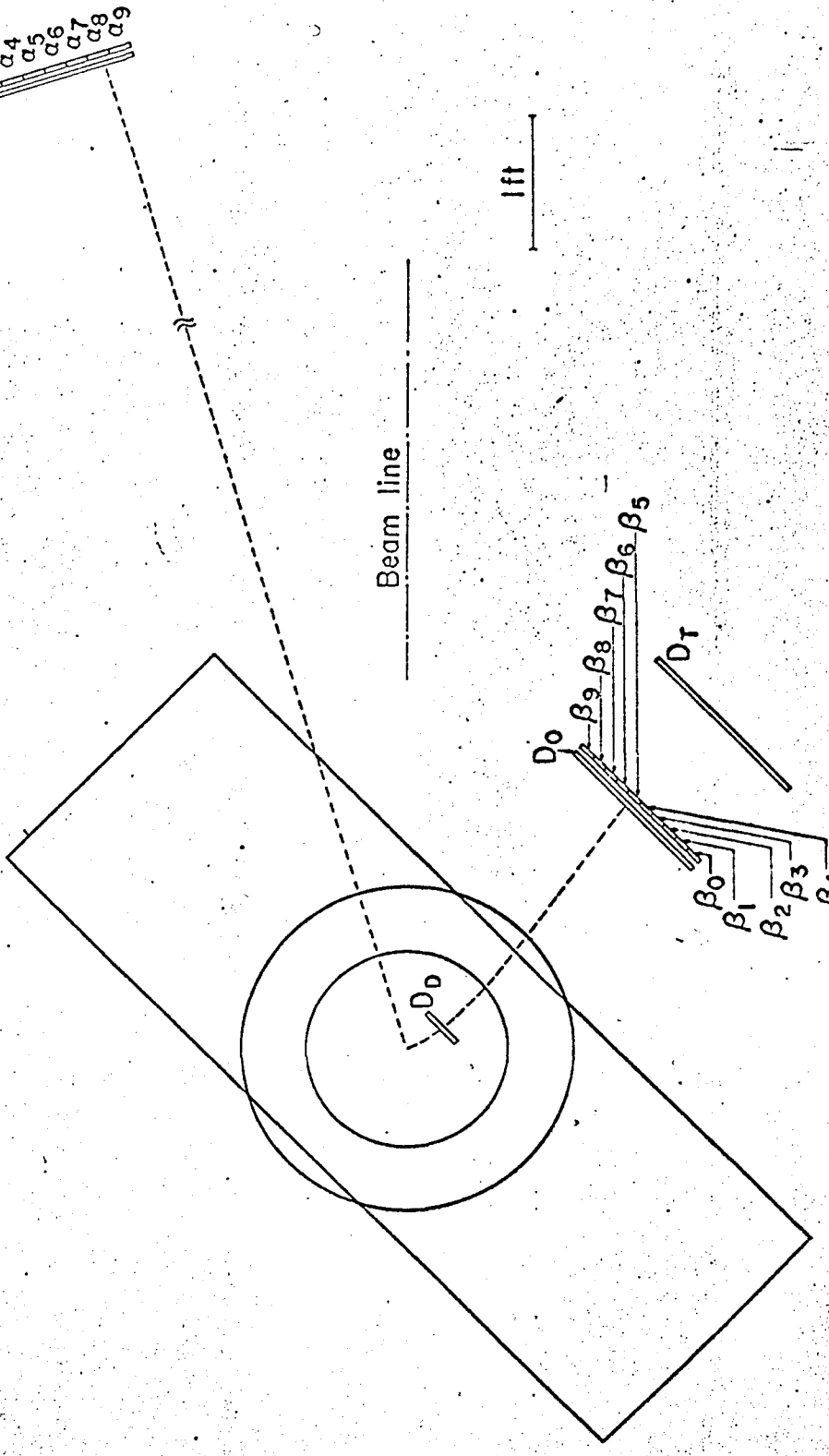
U
a0
a1
a2
a3
a4
a5
a6
a7
a8
a9
1ft
Beam line
β9
β8
β7
β6
β5
Dr
Do
β0
β1
β2
β3
β4
DD

Fig. 4

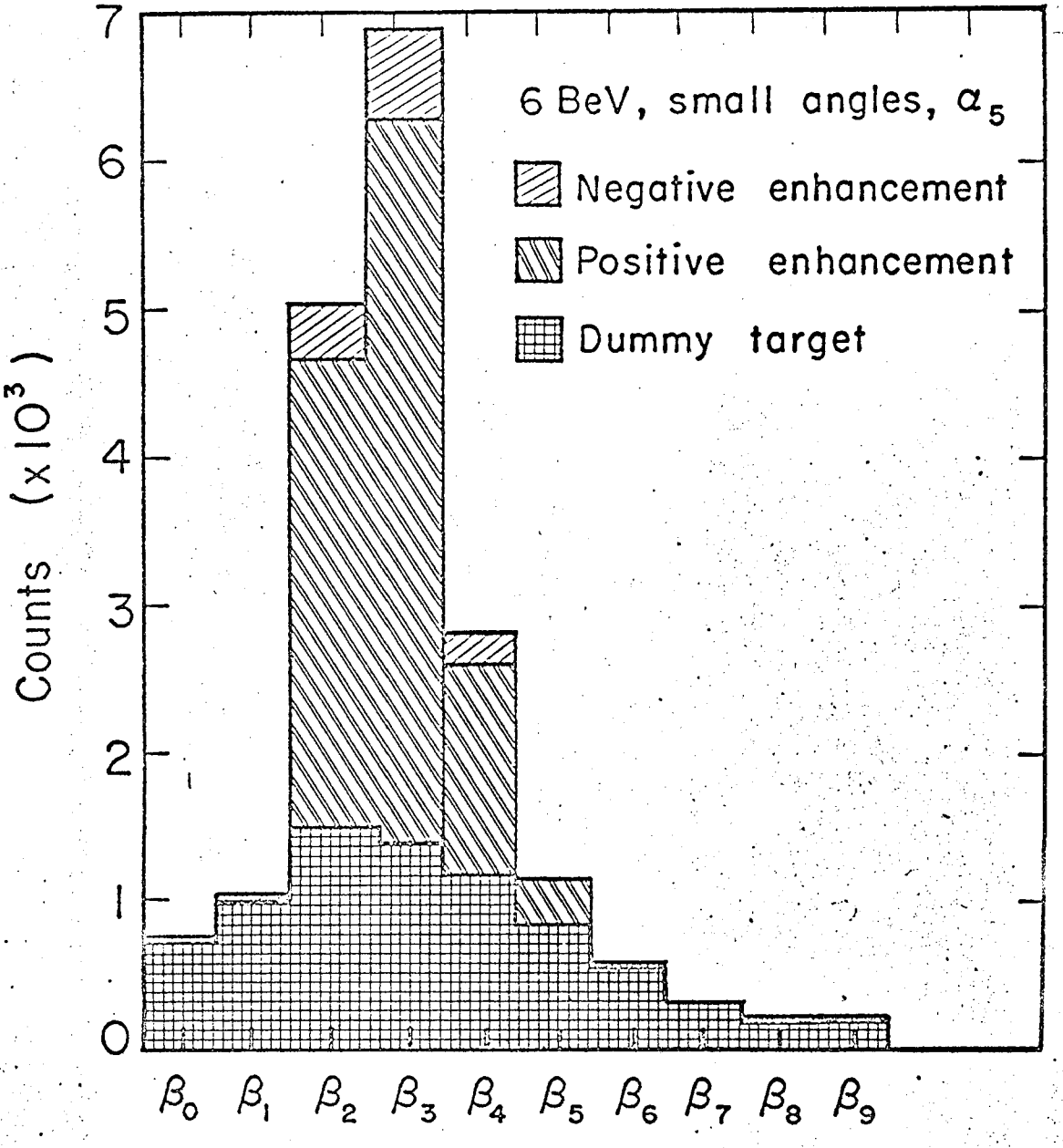

Fig. 5

MU-33098

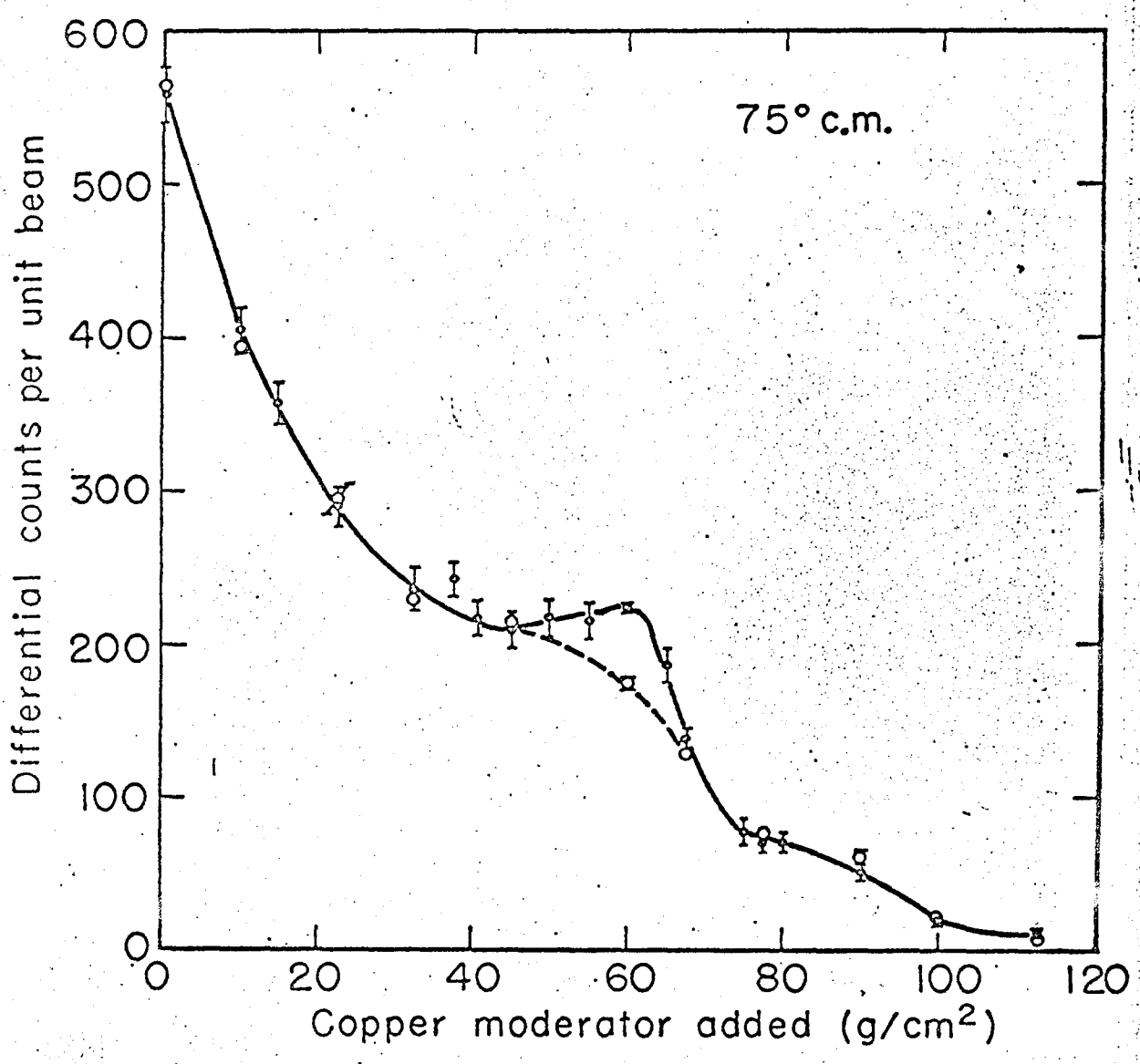

Fig. 6

MU-29815

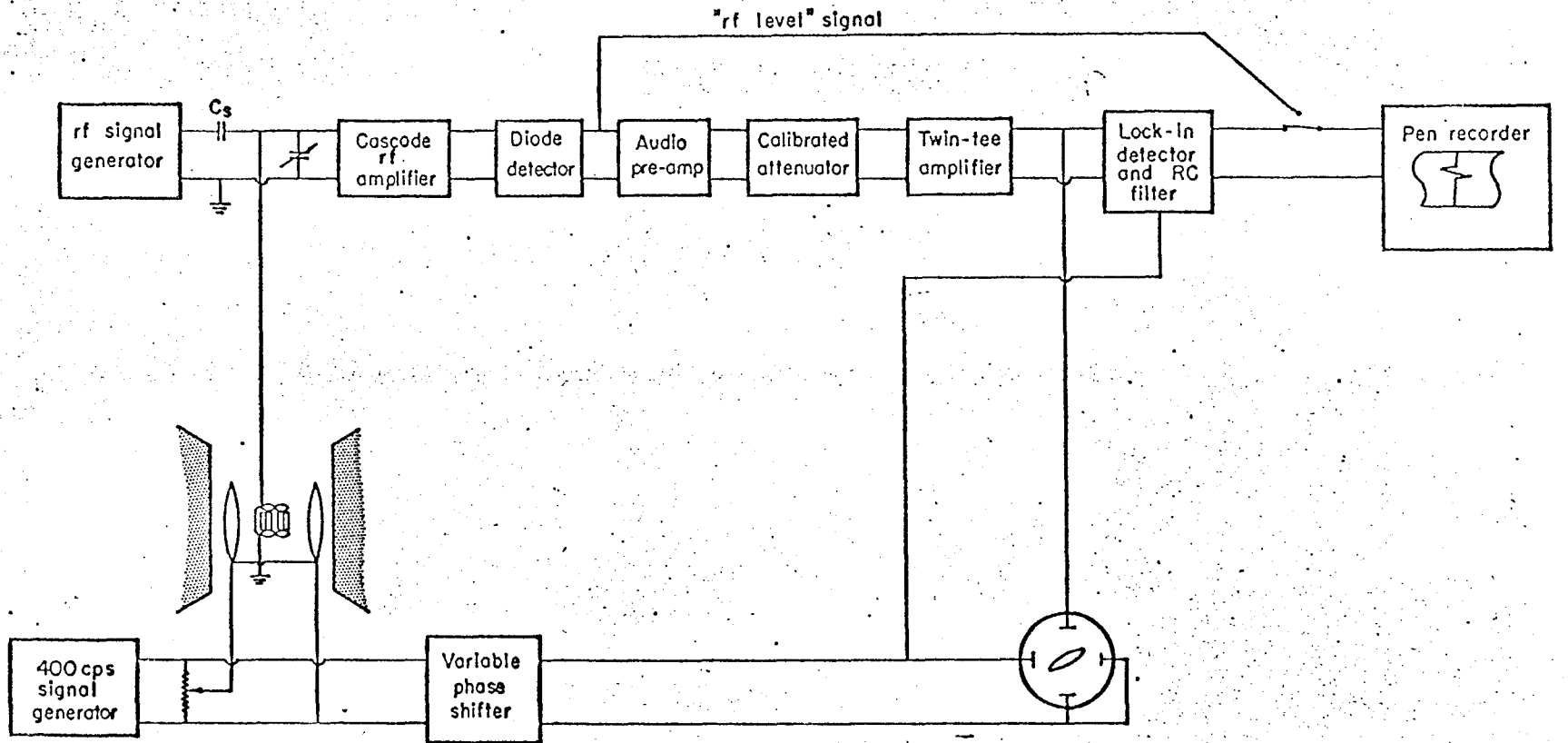

Fig. 7

MUB-2257

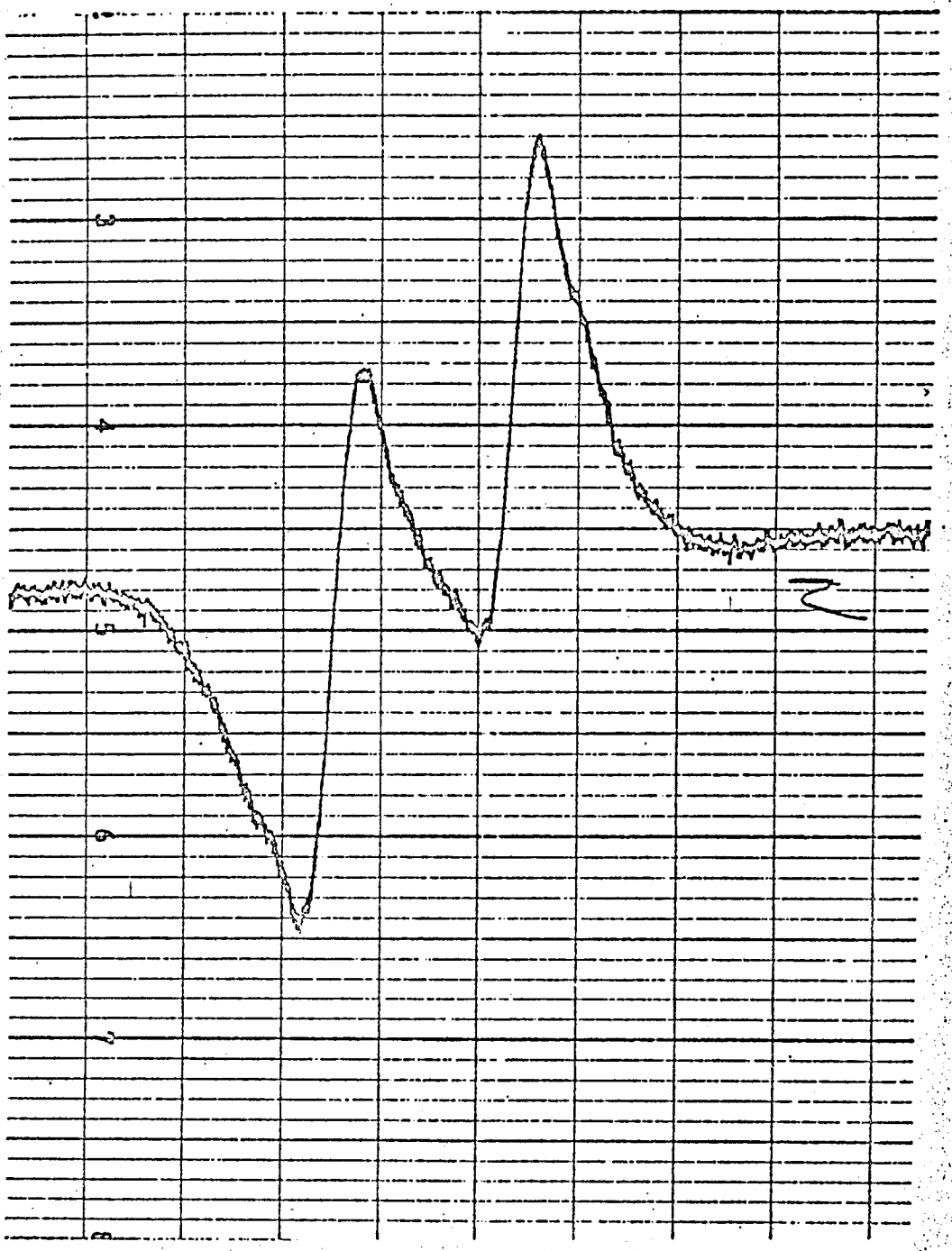

Fig. 8

MU-32736

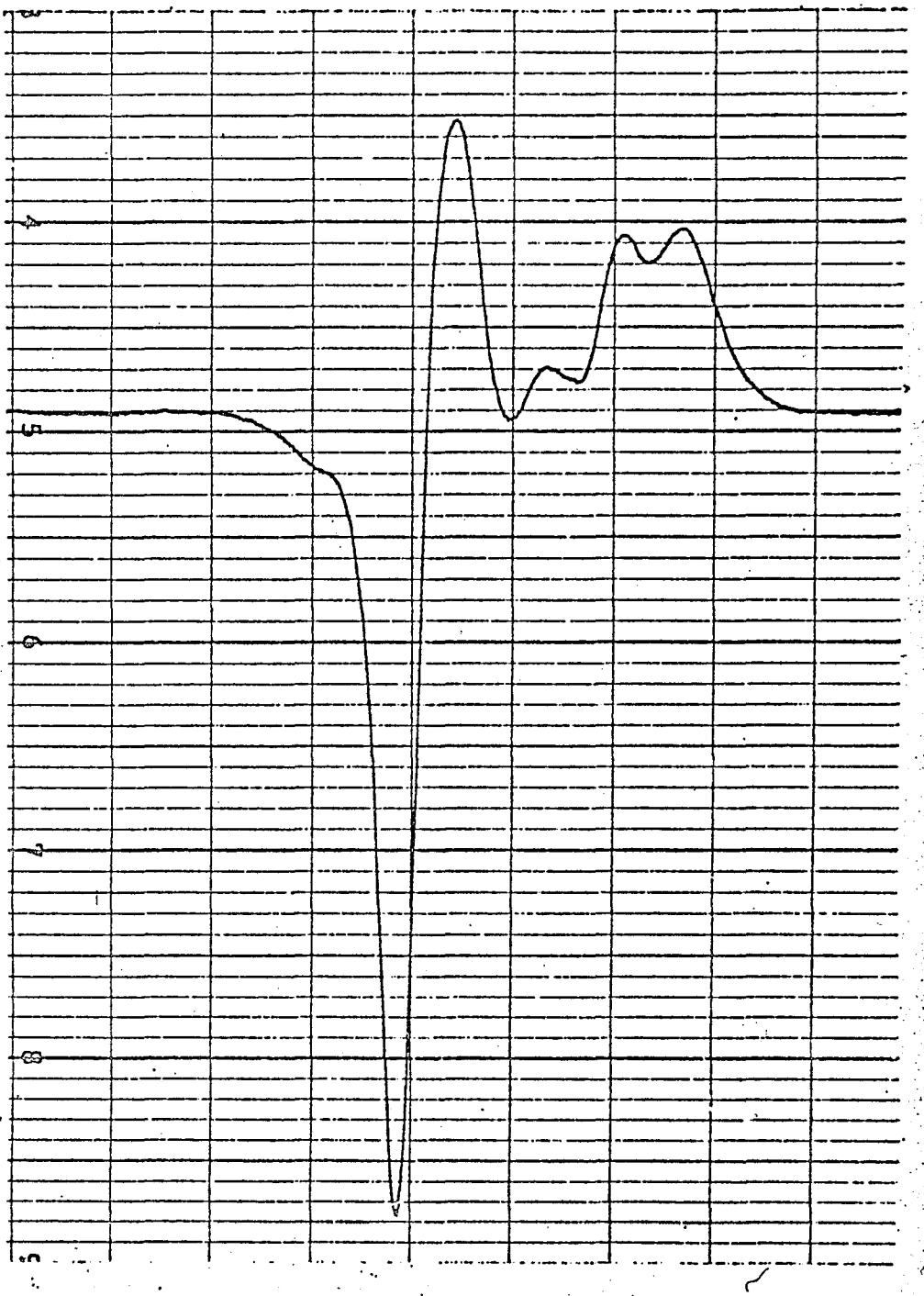

Fig. 9

MU-32735

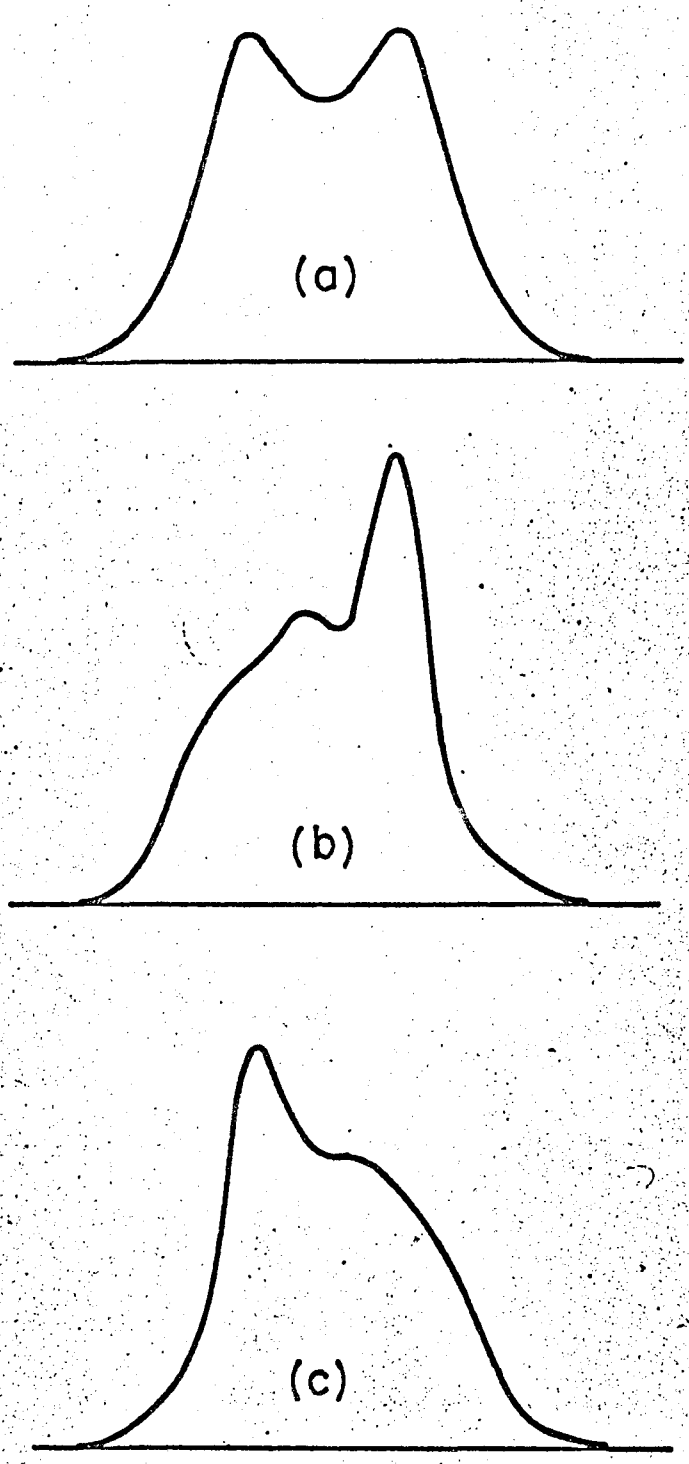

Fig. 10

MU-32816

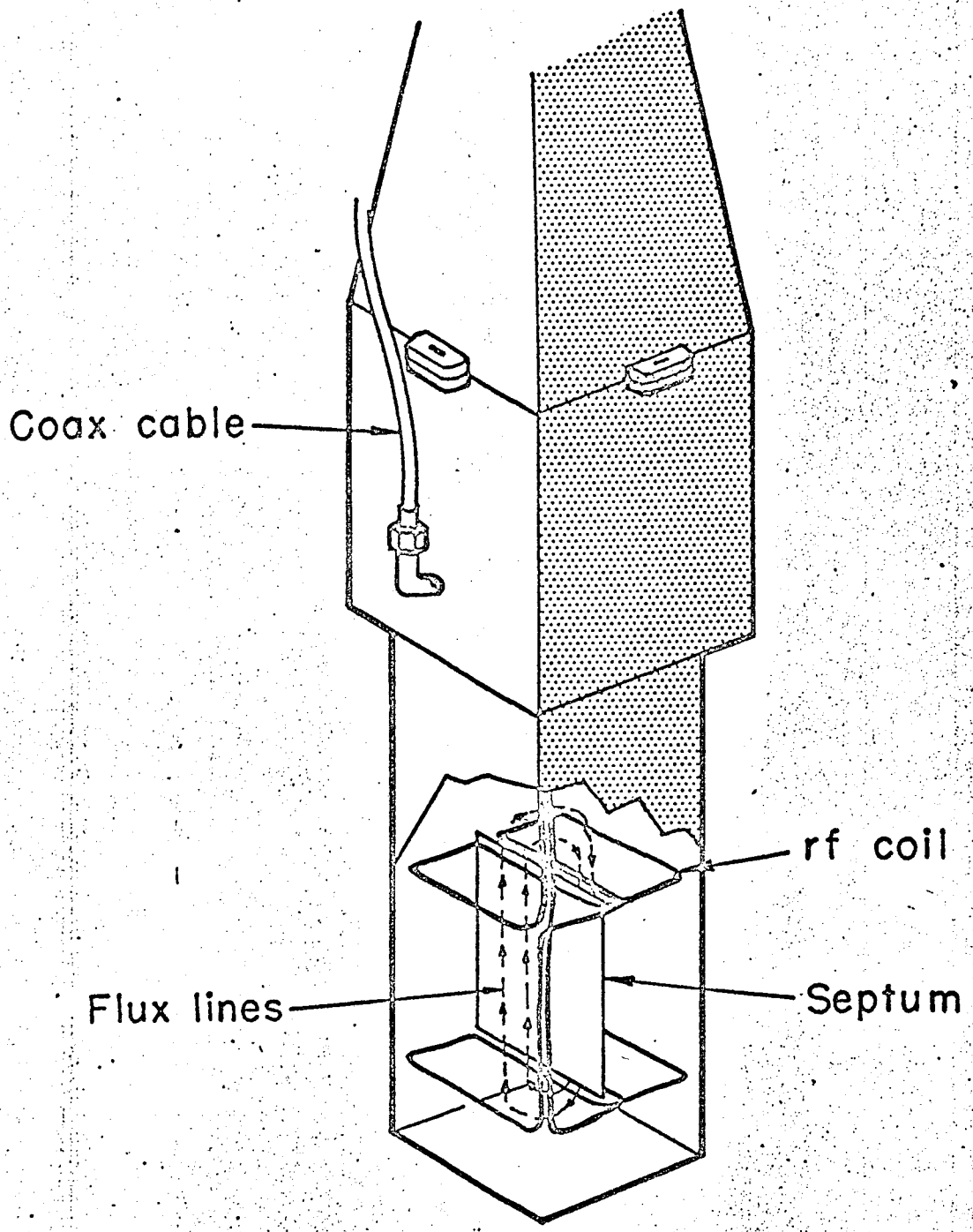

Fig. 11

MU-28653